Journal of Data Acquisition and Processing
ISSN: 1004-9037
https://sjcjycl.cn/
DOI: 10.5281/zenodo.777546

NOVEL CONTROLLER FOR GRID CONNECTED PV SYSTEM THROUGH 13 LEVEL INVERTERS

R.K. Padmashini[1], D. Lakshmi[2]

AMET Deemed to be University

Abstract: Utilization of renewable energy sources is gradually increasing due to soft corner and awareness in public worldwide. Renewable energy sources which are used to produce electricity are becoming popular nowadays since the application of electricity in everywhere. However, in general the generated electrical power from renewable energy sources is depends on nature. Hence, using a single renewable energy source cannot be maintaining reliable power at load. Therefore, integration of two or more different renewable energy sources with an energy storage device is a better idea for supplying quality and reliable power to the load in a standalone system. However, mainly operated loads connected in the distribution system are both single and three phase AC. A three phase inverter is required to provide AC supply from DC to loads at load bus. Usually a multilevel inverter with a proper controller can provide quality power as well as inject fewer harmonic into the load as compared with conventional inverter. A novel control of the 13-level inverter with the help of an artificial neural network is proposed in this paper to supply quality power to the load under various conditions. A multilayer neural structure is considered in this paper to achieve the better response. The hybrid standalone system is simulated on MATLAB platform to obtain required responses for presenting the results in this paper.

Keywords: Hybrid System; Standalone; Power Quality; Multilevel Inverter, ANN.

1. Introduction

The electricity is becoming one of the daily needs to perform various tasks in our daily life. Human life without electricity cannot be imagining and there will be no sufficient growth in present days. In generally a standalone power generation system is used for many applications including rural where power grid is not possible practically, hospitals, armed forces, institutions and many more [1-2]. In such places the diesel generators are unique solution to provide supply. However, the consumption of diesel leads to many problem including cost, pollution and many harmful effects on human life. To overcome these issues, using renewable energy sources for generating required electricity to fulfill the needs is a feasible solution [3].

Due to their availability in many important locations across the world, solar and wind energy are ranked first in the list of sources of green energy. The establishment of a hybrid wind and solar power system can generate stable quality [4]. However, solar energy is not available during night as well as during some cloudy conditions, similarly wind also cannot be available in all the times. Moreover, the loads connected at AC bus are also varying frequently without concern by the generation. Hence, to maintain power balance in the standalone system, energy storage devices like batteries or hydrogen storage systems are needed [1]. In order to ensure correct charging and discharging processes, a battery bank is used in this paper by integrating to dc-link using a bidirectional DC to DC converter. Through proper control of the DC to DC converter and regulation of the battery current in accordance with power imbalance between generation and consumed load in the standalone system, the voltage at the dc-link can be maintained at a certain desired value. To fulfil the loads linked to the AC bus, the inverter must be controlled properly. This work considers a 13 level inverter with an unique control approach to decrease the injected harmonics into the loads connected at AC bus.

The power distribution system often operates with a single phase, three phases, including nonlinear loads. Some loads on the AC bus may use unbalanced currents from the phases or legs of the inverter. Moreover, the nonlinear nature of these unbalanced currents allows them to introduce second frequency (2ω) oscillations into the voltage at the dc-link [4]. The wind turbine's shaft may shake as a result of the "2ω " oscillations in the dc-link voltage, and the heat generated by the PV modules may also increase [1, 5]. The generated power can be decreased by shaft shaking and increased heat at PV modules, respectively. Hence, it is required to eliminate the 2ω oscillation from dc-link through a proper control scheme of the inverter. Thankfully, a 13 level diode bridge inverter features a neutral facility that allows an appropriate controller to cycle unbalanced currents via the inverter leg (phase) to neutral. As well as maintaining balanced voltages under unbalanced load on the AC bus, the controller can also assist in compensating the reactive power required by the load in the meantime.

There are many random changes possible in a hybrid standalone system from both generation and load side. These changes are happens due to nature and load requirement by consumer. Further these random changes even cannot predict properly. Under this situation, the control scheme based on conventional proportional plus integral (PI) controllers will exhibits its poor performance due to rapid changes occurs in the system [6]. Artificial neural network (ANN) based controllers are adopted in this paper to obtain enhanced response of the system through a proposed control scheme under rapid changes. The control of a 13 level inverter proposed in this paper for fulfill the following objectives.

- To establish a two-way oscillation path through the inverter legs and neutral.
- To compensate for the reactive power required by the load and reduce the harmonics fed into the load bus.
- To use ANN controllers to provide a quick response under changing conditions.
- To keep balanced voltages at the AC bus while unbalanced currents are flowing via the three phase legs.
- To enhance the power quality at the AC bus with suggested 13 level inverter control.

Further the paper is organized by providing detailed description of the system along with literature survey in Section-2. The designing of a multilayer ANN is prepared in the Section-3. The control schemes of DC and AC side are discussed in Section-4In MATLAB. Results from Simulink are discussed in Section 5's case studies. The list of references is provided at the end of the article, which is followed by the conclusion section.

2.About the Standalone System

The PV system, wind power generation, corresponding MPPT converters, battery bank, bidirectional dc to dc converter, AC loads, and 13 level inverter make up the hybrid standalone system seen in Fig. 1. Their renewable energy sources (PV and wind) can be operated at their maximum power level with the use of individual MPPT devices. The boost converters are used as MPPT converters due to its ability to pump the current into dc-link under availability of low power generation also [7]. The battery should react appropriately when there is a power imbalance between the load connected to the AC bus and the generation. Typically, the power difference between the generation and the load will determine the voltage at the dc-link. So, to maintain power balance by adjusting voltage at the dc-link, a bidirectional dc to dc converter is utilized between the battery and dc-linkAn inverter is needed to convert the DC supply to AC in order to fulfil the loads attached to the AC bus. Unfortunately, traditional inverters introduce harmonics into the AC bus, leading to problems with power quality. Moreover, loads linked to the AC bus typically combine single and three phase power. A 13 level inverter is mostly preferable for medium power ranges especially in distribution system due to its many advantageous in terms of the performance, size and economical issues [8-10]. Therefore, a three phase 13 level inverter with a novel controller is incorporated between dc-link and AC bus through a filter. Due to a standalone system, it is crucial to manage both the frequency and voltage at the AC bus. In this research, an appropriate inverter control mechanism is used to give high-quality power to the AC bus. When generating the necessary pulses for the inverter, the space vector pulse width modulation (SVPWM) mechanism is more common than other methods [11]. The harmonics added to the AC bus can be reduced with the help of the SVPWM technique. By keeping the voltage at the dc-link constant, the inverter may regulate the voltage at the AC bus. In order to preserve the quality of the power at the AC bus, it is necessary to describe the control strategy of the bidirectional dc to dc converter.

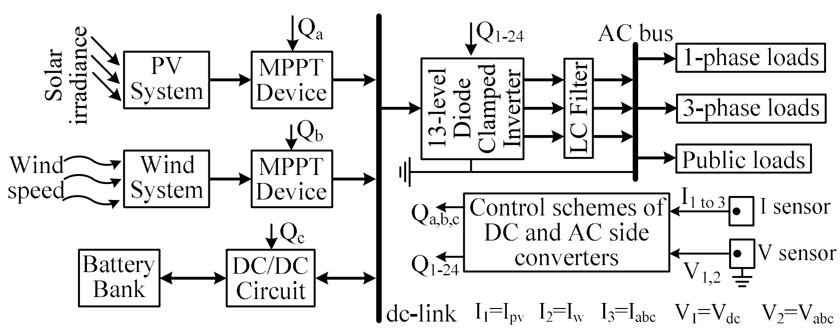

Fig. 1:

The modeling of the major components involved in the Fig. 1 is provided in this section for a better analysis of the system.

The designing of a three phase LC filter is attempted with the help of below equations [12]:

$$k = \left(\frac{k^2 - \frac{15}{4}k^4 + \frac{64}{5\pi}k^5 - \frac{5}{4}\mathrm{k}^6}{1440} \right)^{1/2} \quad (1)$$

$$Lf = \frac{Vo}{Iofs}\left\{K\frac{Vdc}{Vo,av}\left[1+4\pi^2\left(\frac{fr}{fs}\right)^2 K\frac{Vdc}{Vo,av}\right]\right\}^{1/2} \quad (2)$$

$$Cf = K\frac{Vdc}{Lffs^2Vo,av} \quad (3)$$

where, the modulation index is represented by term 'k'. The voltage at load bus and load current are considered as V_o and I_o respectively. The output frequency and switching frequency are denoted as f_r and f_s respectively. The factor of total harmonic load voltage is taken as $V_{o,av}$ (i.e., <5% of V_o). The filter parameters such as inductance and capacitor are obtained as L_f and C_f.

The basic d-q reference frame equations are used in this study to simulate the permanent magnet synchronous generator (PMSG) coupled two mass model of a wind turbine [13–14].

$$2Ht\frac{d\omega_t}{dt} = T_m - T_{sh} \quad (4)$$

$$\frac{1}{\omega_{elb}}\frac{d\theta_{tw}}{dt} = \omega_t - \omega_r \quad (5)$$

$2H_g($

$$2H_g\frac{d\omega_r}{dt} = T_{sh} - T_g \quad (6)$$

where, H_t and H_g are represents inertia constant of the turbine and generator respectively. ω_t is the angular speed of the wind turbine and θ_{tw} is the shaft twist angle, ω_r is the rotor speed of the generator and ω_{elb} is the electrical base speed. Hence the shaft torque T_{sh} is expressed by

$$T_{sh} = K_{sh}\,\theta_{tw} + D_t\frac{d\,\theta_{tw}}{dt} \quad (7)$$

where, K_{sh} is the shaft stiffness and D_t is the damping coefficient.

Parameters of Two Mass Drive Train [1]

H_t	4s
H_g	0.1H_t
K_{sh}	0.3 p.u./el.rad
D_t	0.7 p.u.s/el.rad

Parameters of PMSG [1]

Number of poles	10
Rated speed	153 rad/s
Armature resistance (R_s)	0.425 Ω
Magnetic flux linkage	0.433 Wb
Stator inductance (L_s)	8.4 mH
Rated torque	40 Nm
Rated power	6 kW

The PV module is modelled by the basic equation of the PV cell which expressed in blow function [15].

$$I_{pv} = I_{ph} - I_{rs}\left[\exp\left(\frac{q\left(V_{pv} + I_{pv}R_s\right)}{AKT}\right) - 1\right] - \frac{\left(V_{pv} + I_{pv}R_s\right)}{R_{sh}} \tag{8}$$

where, $I_{rs} = I_{rr}\left[\frac{T}{T_r}\right]^3 \exp\left(\frac{qV_D}{AK}\left[\frac{1}{T_r} - \frac{1}{T}\right]\right), I_{ph} = \left[I_{sc} + k\left(T - T_r\right)\right]\frac{G}{1000}$

where q=1.602·10^{-19} C is the electron charge, K=1.3806·10^{-23} J/K is Boltzmann's constant, A=2 is the p-n junction's idealistic factor, T is the cell's temperature (K), T_r is the reference room temperature (K), I_{ph} is the cell's photocurrent (it depends on the solar irradiation and temperature), I_{rs} is the cell's reverse saturation current, G is the solar irradiance and V_{pv} is cell voltage V_D is the voltage across the diode, R_s is cell internal series resistance, R_{sh} is cell shunt resistance, k is the short circuit current-temperature factor, and I_{pv} is cell current.

The model diagram of a PV cell and respective PV array by connecting cells in the combination of series and parallel is shown in Fig. 2. In Fig. 2, I_{PV} and V_{PV} are the PV array's current and voltage respectively. The voltage based modeling of the PV array is depicted in Fig. 3. While the doing modeling of the PV system, considered 'n_p' number of cells connected in parallel and n_s number of modules connected in series. The listed parameters of PV systems are depicted in Table-3.

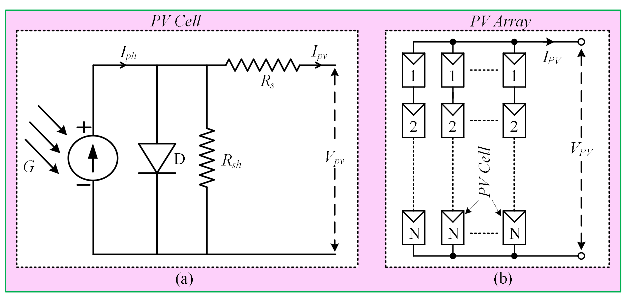

Fig. 2: Schematic Diagram of (a) PV Cell and (b) PV array

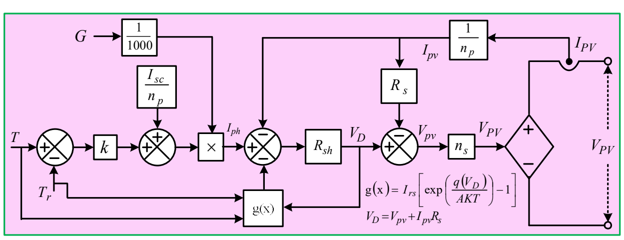

Fig. 3: Detailed modeling of PV array

Table-3: Parameters of PV

Open circuit voltage of module V_{oc}	36.90V
Short circuit current of module I_{sc}	8.01A
Voltage at maximum power V_{mpp}	30.3V
Current at maximum power I_{mpp}	7.10A
Series resistance R_s	0.0045

Shunt resistance R_{sh}	0.9822
Cell diode voltage V_D at MPP V_{dm}	0.5367
No. of cells connected in parallel/module	Vary*
No. of cells connected in series/module N_s	Vary**
Reference room temperature T_r	25^0C
Cell thermal voltage V_t	26mV
PN-junction diode current at MPP	0.3636
Reverse saturation current I_{rr} at $T=T_r$	$3.94\text{x}10\text{-}^{-10}$
PN-junction diode voltage at MPP V_{dm}	0.5367
Number of modules connected in series n_s	22
Rated irradiance G*	1000W/m^2
Rated power of PV array	4.73kW

Note: Calculations of PV parameters:

Ns=Round (V_{oc}/0.61)

$$I_{dm} = I_{sc} - I_{mpp} - \frac{V_{dm}}{R_p} \tag{9}$$

$$I_{rr} = \frac{\left(I_{sc} - \frac{V_{oc}}{N_s R_{sh}}\right) \Big/ \left(\exp\left(\frac{V_{oc}}{N_s V_t}\right) - 1\right)}{\left[\frac{T}{T_r}\right]^3 \exp\left(\frac{qV_D}{AK}\left[\frac{1}{T_r} - \frac{1}{T}\right]\right)} \tag{10}$$

$$V_{dm} = V_t \times \log\left(I_{dm} / I_{rr} + 1\right) \tag{11}$$

$$R_s = \frac{\left(V_{dm} - \frac{V_{mpp}}{N_s}\right)}{I_{mpp}}, \quad R_{sh} = \frac{\left(\frac{V_{mpp}}{N_s I_{mpp}} - R_s\right) \times R_p}{\left(R_p - \frac{V_{mpp}}{N_s I_{mpp}} + R_s\right)} \tag{12}$$

$$I_{pt} = \frac{V_t}{R_{sh}}, \quad R_p = \frac{V_{dm}}{\left(I_{sc} - I_{mpp} - I_{pt}\right)} \tag{13}$$

While calculating above parameters, the initial values needs to be fixed first and the process should repeat at least 10 iterations to get accurate values. The initial parameters are

$R_p = 100 \times \frac{V_{oc}}{N_s I_{sc}}$ and $V_{dm} = \frac{V_{oc}}{N_s}$

The modeling of the battery bank is very important since battery should able to manage energy management system under any conditions. The temperature and SoC of the battery is also included to obtain the realistic responses. An electrochemical model of a lead acid battery is developed in this paper with the help of below basic equations [1, 16-17].

$$E_m = E_{m0} - K_E\left(273 + \theta\right)\left(1 - SOC\right) \tag{14}$$

$$Q_e(t) = Q_{e\_init} + \int_0^t -I_m(\tau)d\tau \tag{15}$$

$$I_p = V_{PN} G_{P0} \exp\left(\frac{V_{PN}}{V_{P0}(\tau_P s + 1)} + A_P \left(1 - \frac{\theta}{\theta_f} \right) \right) \tag{16}$$

$$C(I,\theta) = \frac{K_c C_{0*} K_t}{1 + (K_c - 1)(I/I^*)^{\delta}}, K_t = LUT(\theta) \tag{17}$$

$$SOC = 1 - \frac{Q_e}{C(0,\theta)}, \quad DOC = 1 - \frac{Q_e}{C(I_{avg},\theta)} \tag{18}$$

$$\theta(t) = \theta_{init} + \int_0^t \frac{\left(Ps - \frac{(\theta - \theta_a)}{R_\theta} \right)}{C_\theta} d\tau \tag{19}$$

where, E_m is the open-circuit voltage (V), E_{m0} is the open circuit voltage at full charge (V), θ is electrolyte temperature (^{0}C), Q_e is the extracted charge (A S), Q_{e_init} is the initial extracted charge (A S), I_m is the main branch current (A), τ is an integration time variable, I_P is the current loss in parasitic branch, V_{PN} is the voltage at the parasitic branch, τ_P is a parasitic branch time constant, θ_f is electrolyte freezing temperature (^{0}C), C_{0*} is the no-load capacity at 0^0C, K_t is a temperature dependent look-up table, I^* is a nominal battery current, DOC is a depth of charge, C is the battery capacity (A) , K_E, G_{P0} and δ are constants.

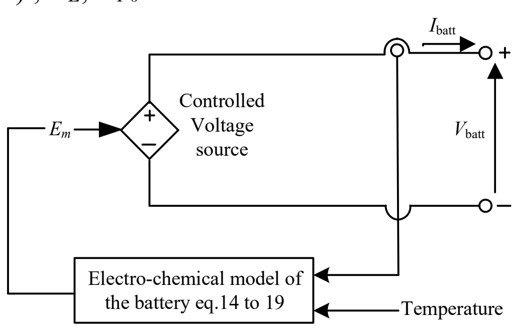

Fig. 4: Model of a battery bank

A proper rating of the battery bank should be required to make the better operation of a standalone system. By considering 60% of the SoC under the assumption that even when the solar and wind power is zero it should cater to the energy requirement of a 16kW load for approximately an hour.

Calculation for battery rating = $\frac{16\,kW \times 1\,hr}{300\,V \times 0.6} = 88.88$ Ahr

2. Multilayer ANN

The PI controllers are unable to produce accurate output during rapid changes due to its fixed gains which tuned at particular instant [6]. To avoid this issue, an ANN is used where the gains can be updated in online through training mechanism for any random changes in the system. However, a multilayer perceptron based ANN can produce stable and accurate output under any instant of variations in input [18-19]. Hence, multilayer based ANN is required while deigning control schemes of both dc to dc converter and inverter. The error signal of a controller can be considered as input to the ANN controller. The architecture of a simple multilayer ANN controller is shown in Fig. 5. Two input nodes ($N_{1,2}$) are considered for error and change in error as inputs. The hidden nodes with activation function are represented by 'H_{nm}'. The hidden nodes without activation function are represented by 'F_n' where 'n' represents number of nodes and 'm' represents number of hidden layers. An error back propagation technique is used to update the input weights. This designed and trained ANN controller is further used in control schemes of dc to dc converter and inverter to obtain the better response.

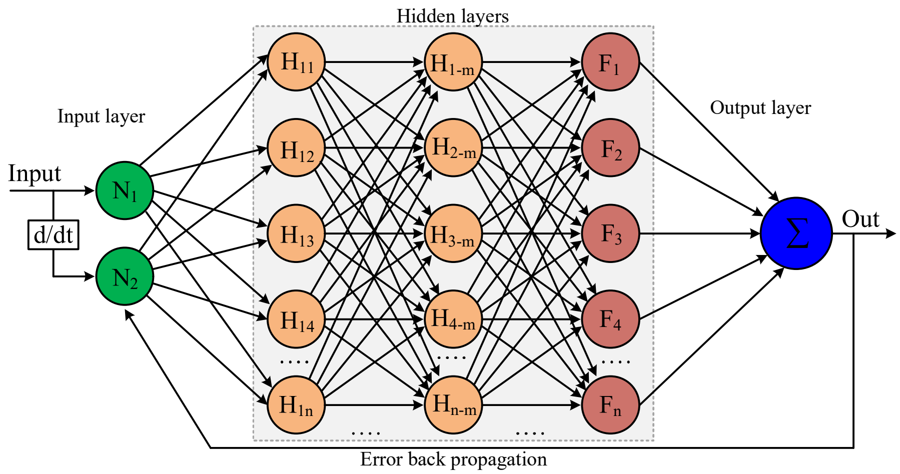

Fig. 5: Multilayer ANN architecture

3. Control schemes of voltage at dc-link and AC bus

The energy management system can be implemented on the basis of regulating voltage at dc-link since the power balance between generation and load reflected by the dc-link voltage. The voltage at dc-link will be fall down if load at AC bus demanding more than the generation by renewable energy sources. In the other side, the voltage can be raise if the load demand at AC bus is less than the total generation from the renewable energy sources. Therefore the power balance is achieved by controlling the dc-link voltage at its reference value through regulating the charging and discharging current of the battery bank. The charging and discharging process of the battery current can be done by bidirectional dc to dc converter with the help of proper control strategy. The bidirectional dc to dc converter is designed by using two switched where one switch used for charging and another for discharging.

The battery can be charged more quickly by maintaining its voltage lower than the dc-link voltage. In order to get the fastest charging possible by regulating it, one switch can act as a buck converter. In a similar manner, the battery discharge process is accomplished by raising the voltage to the dc-link reference signal by using another switch as a boost converter. To maintain the dc-link voltage at its reference, two switches () can convert the bidirectional converter into a buck-boost converter. Fig. 6 depicts the suggested control scheme for the bidirectional dc to dc converter. The controller is created without taking into account the battery current in order to reduce the number of sensors. To prevent the battery from being overcharged or discharged, the state of charging (SoC) of the battery is taken into account when constructing the control scheme. A trained ANN controller determines the needed duty cycle by comparing the voltage at the dc-link to its reference signal.

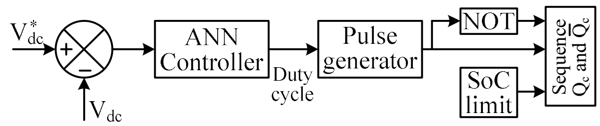

Fig. 6: Control scheme of dc to dc converter for voltage at dc-link.

Once the bidirectional dc to dc converter has produced a consistent dc-link voltage, the inverter is in charge of supplying quality power to the AC bus. The fluctuations in frequency at the AC bus might be brought on by the active power required by the load. In order to create the reference active component of current using an ANN controller, the frequency at the AC bus is compared to the reference frequency. Moreover, this "2ω" component is compared to zero to produce an oscillating component that is equal in the direct axis current through the PI controller. As a result, oscillations in the voltage at the dc-link are eliminated by forcing the inverter legs to circulate the "2ω" oscillations. Similar to how the reference current signal of the quadrature axis is obtained, the RMS voltage of the signal is compared to the reference value using an ANN controller. Both the reactive power and the RMS voltage at the AC bus can be kept constant with the aid of this. Once obtained the reference values of current in DQ form, these are compared with the actual DQ current which are obtained from 3-phase load current to generate required voltage components through ANN controllers. To make the decoupling action, the filter components also added. The required pulses are generated through SVPWM technique by using the reference signals of DQ components of voltages. The proposed inverter control scheme is shown in Fig. 7.

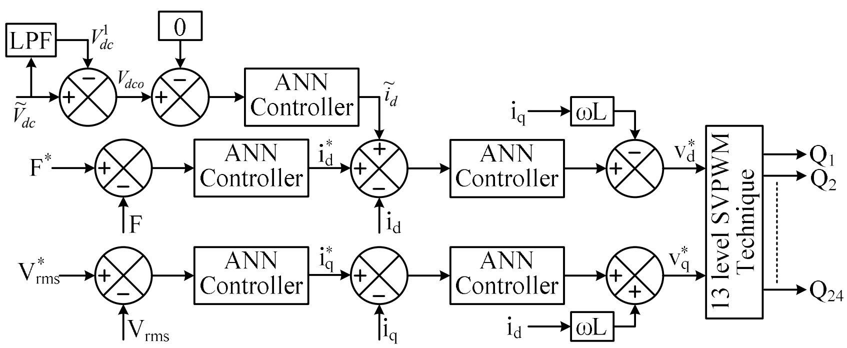

Fig. 7: Proposed control scheme of the inverter

4. Results and Discussions

The proposed controllers for the hybrid standalone system shown in Figure 1 are simulated using the MATLAB platform. This part carries out responses in various circumstances for in-depth talks.

Case-1: Operation with only wind power and load

Every day at night, no electricity will be generated by PV panels. Due to clouds especially during the rainy season, this phenomenon can also happen during the day. In these conditions, the wind generation and battery should be the only sources of the necessary power to the loads. Depending on the operation, the operated loads may be balanced or unbalanced at the AC bus.

The following alterations are taken into consideration in order to get different answers in this scenario (Fig. 8(a) and (b)).

Load:

For 2-3s, load current = 7.4 A

For 3-6s, load current = 3.7 A

Wind Speed

Wind speed = 12 m/s during t=0-2.5s.

Wind speed = 7 m/s during t=2.5-5.0s.

Wind speed = 15 m/s during t=5.0-6.0s.

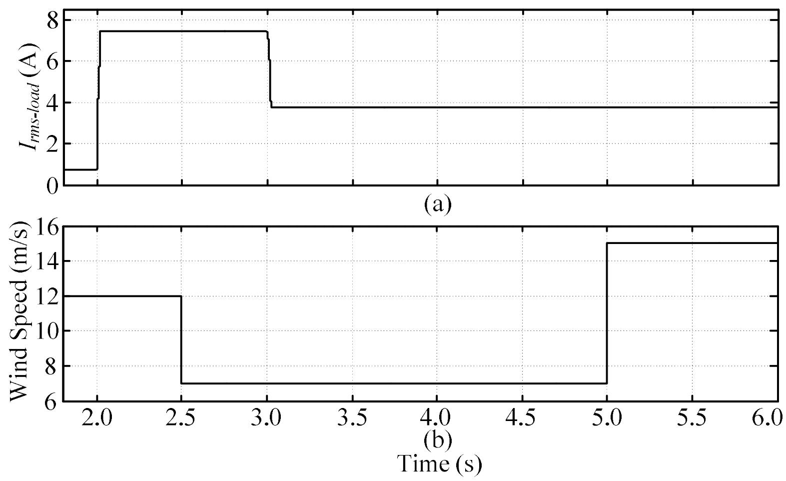

Fig. 8: Variations in (a) Load current, (b) wind speed {*Case-1*}

Fig. 9 shows the dynamic response of the voltage at the dc-link to the aforementioned adjustments. According to Fig. 9, the control strategy of the dc to dc converter can regulate the dc voltage well in both transient and steady state conditions. Furthermore, it can be demonstrated that unlike load change, the dc voltage transient is essentially nonexistent when there is a difference in wind speed. The output ac voltage, however, experiences a transient as a result of the load's change because the load is directly connected to the inverter. Although the RMS value may not provide a clear image during transients at t=3s and it was found that there were few fluctuations in voltage during load transients, the instantaneous single phase voltage at the AC bus is shown in Fig. 10. In all three phases' voltages, the total harmonic distortion (THD) is measured to be less than 1%. The instantaneous load current is also shown in Fig. 11, and it was found that the load may still get sufficient current and voltage during transients. Fig. 12 displays the many powers involved in this case study. Fig. 12 shows that the battery either gives or absorbs power depending on the demand.

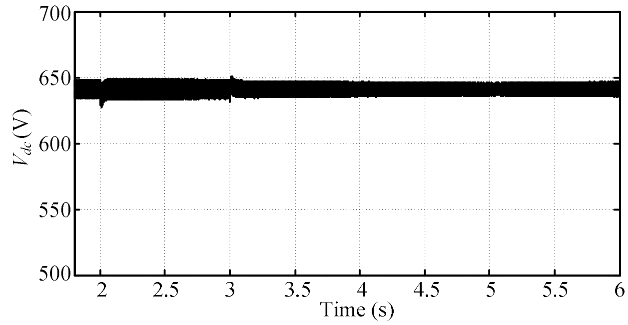

Fig. 9: Voltage at DC-link {*Case-1*}.

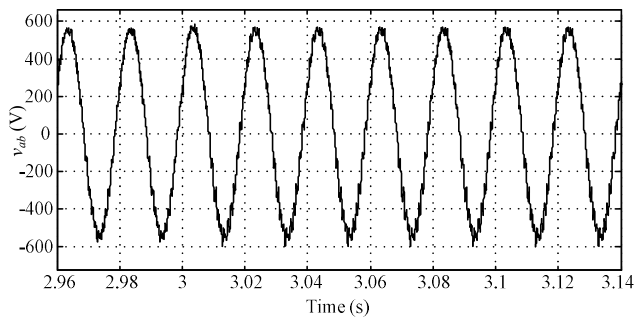

Fig. 10: Instantaneous voltage at t= 3s. {*Case-1*}.

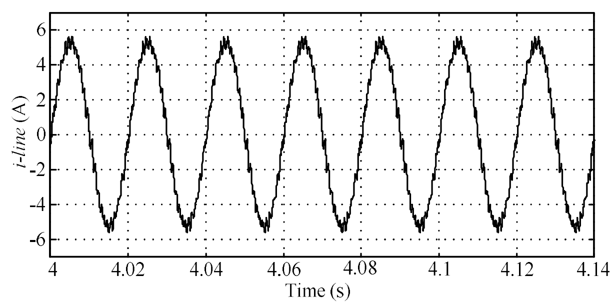

Fig. 11: Instantaneous line current {*Case-1*}.

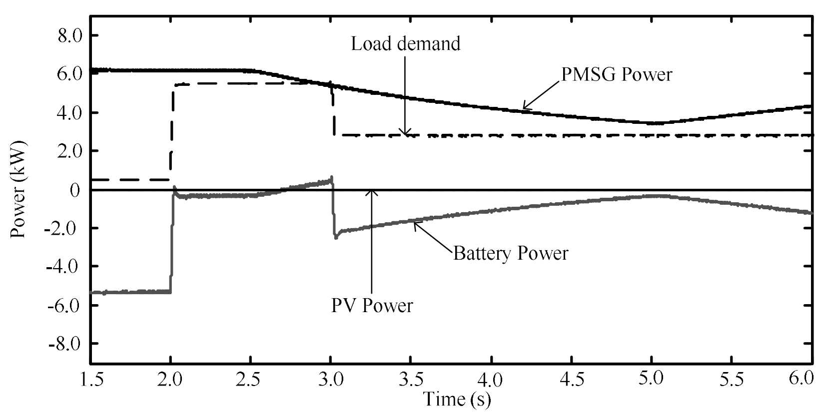

Fig. 12: Powers {*Case-1*}.

Comparing the proposed control of the inverter with the current method, however, can make the response of the RMS voltage more obvious. In Fig. 13, the dynamic RMS voltage responses of the proposed and the one indicated in [20-21] are contrasted when the load changes.

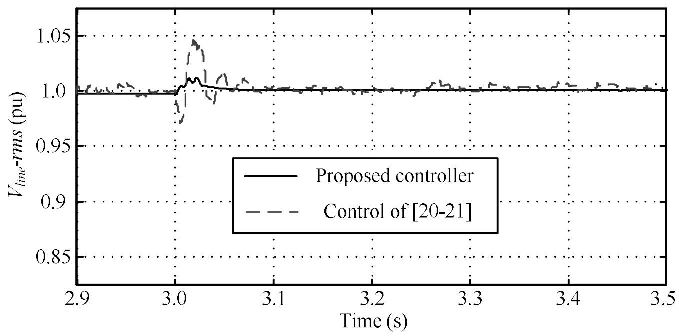

Fig. 13: Response of controllers {*Case-1*}.

Case-2: Responses under unbalanced load at AC bus

The following unbalanced line currents depicted in Fig. 14 are considered in this case to obtain various responses of the standalone system with proposed controllers.

i_{la} = 3.53A;

i_{lb} = 9.55A;

i_{lc} = 8.45A

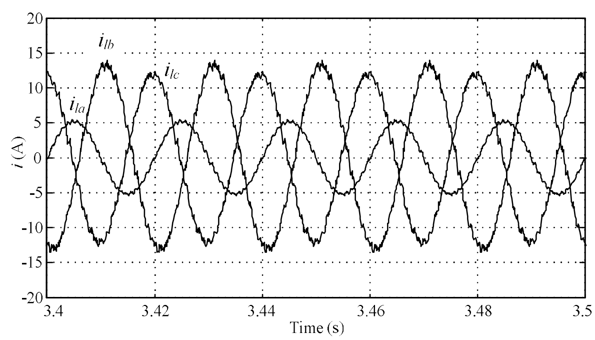

Fig. 14: Three phase currents for unbalanced load {*Case-2*}.

Due to the imbalanced currents, pulsations will occur in the generator's torque. The pulsations must be decreased in order to extend the shaft's fatigue life. Fig. 15 shows the reaction of the PMSG torque with and without the proposed controls. Furthermore, because of imbalanced drops across the filter, the voltages at the AC bus will get out of balance. Yet, as shown in Fig. 16, the suggested controller can keep balanced voltages at the AC bus. By generating various modulation indices for the three legs of a 13 level inverter and adding an oscillating component of direct axis current, the control of the inverter is able to maintain balanced RMS voltages. Fig. 17 shows the corresponding RMS voltages and associated modulation indices.

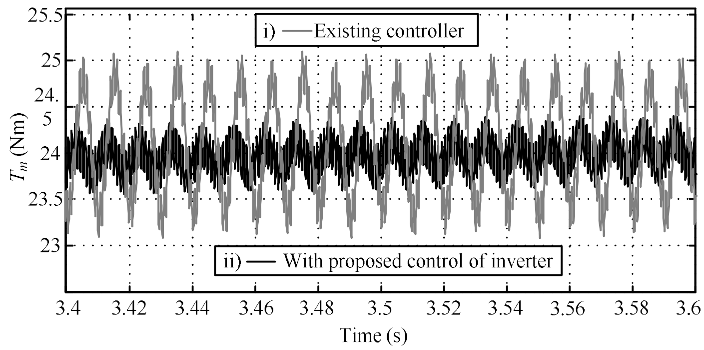

Fig. 15: Electromagnetic torque of generator with and without proposed controller {*Case-2*}.

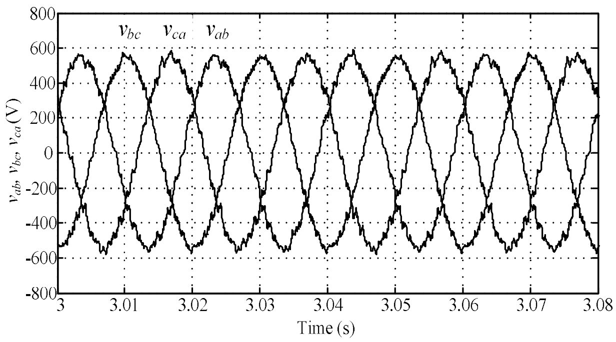

Fig. 16: Instantaneous line voltages at AC bus with proposed control of inverter {*Case-2*}.

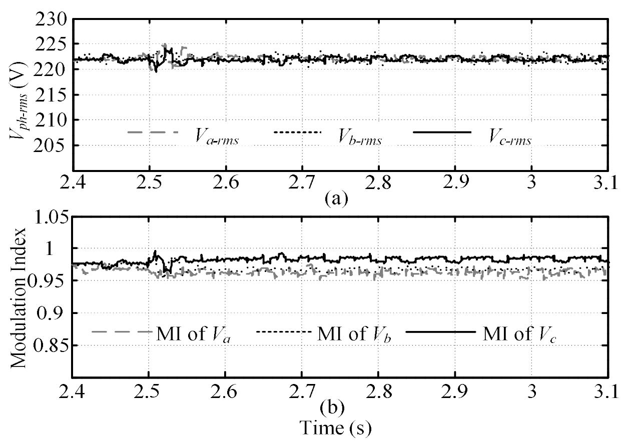

Fig. 17: (a) line voltage RMS; (b) 3-phase modulation indexes {*Case-2*}.

Case-3: changes in sources and load

The solar irradiance and wind speed will typically fluctuate, and the changes in load may not be precisely predicted at the same time. In order to assess the responses of the inverter and dc to dc converter of the battery, random changes in load, wind speed, and solar irradiance are taken into account. A 15-hour time pattern is taken into account for all the patterns in order to provide a realistic representation. Fig. 18 depicts the alterations taken into consideration in this scenario. If 0 seconds is the time at 7 in the morning, and 15 seconds is at 10 at night, is how the time scaling factor is employed in Fig. 18. Fig. 19 shows the dynamic response of the battery to load and overgeneration. According to Fig. 19, the controllers operate satisfactorily in all situations.

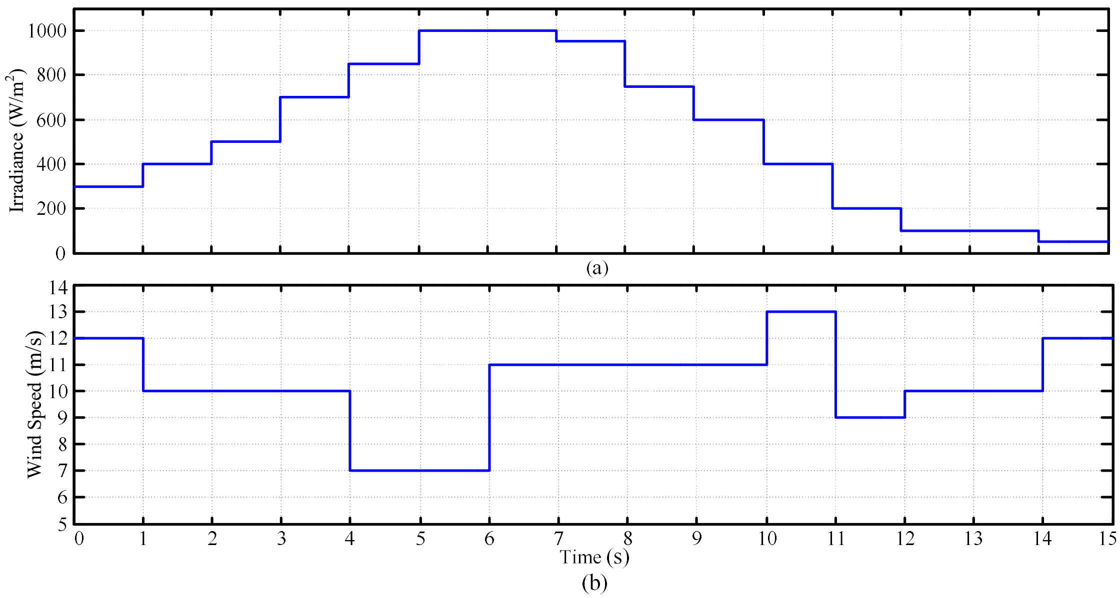

Fig. 18: changes in (a) irradiance, (b) wind speed {*Case-3*}.

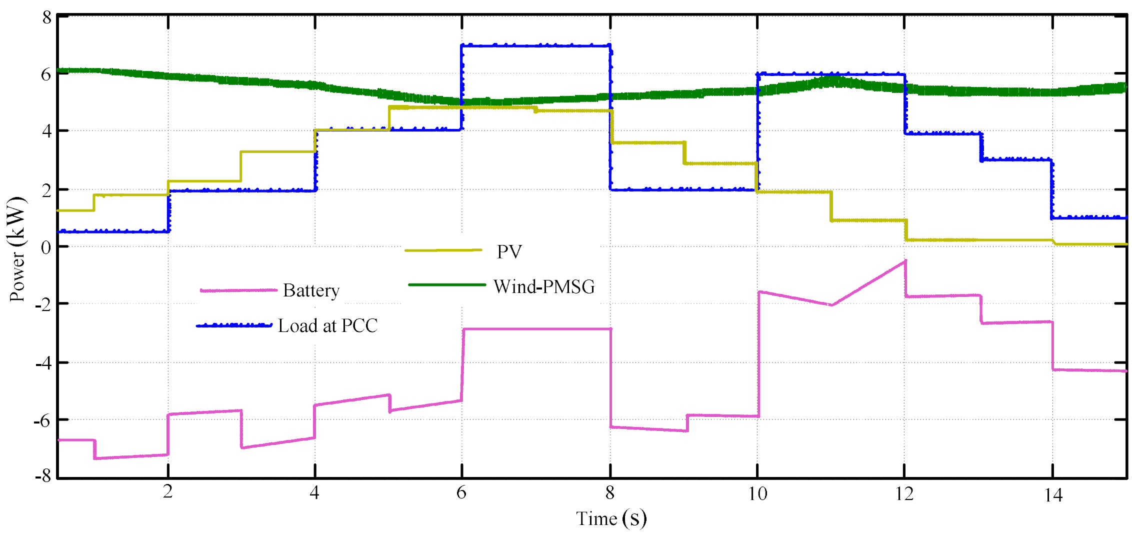

Fig. 19: various powers {*Case-3*}.

5. Conclusion

Proposed controllers of the standalone hybrid renewable energy sources system with a 13 stage inverter improve the power quality. To lengthen the fatigue life of the wind turbine shaft and lower the heat across PV panels, the second frequency oscillation component is removed from the voltage at dc-link. A good LC filter is made to enhance the voltage profile. With the SVPWM approach, AC loads can respond quickly while receiving less harmonics. To maintain the system's energy management, the bidirectional dc to dc converter and battery are connected to a control scheme. By using the suggested inverter controller, the voltage and frequency at the AC load are both kept at their reference values. To get the valuable replies, ANN-based control techniques are used. In this paper, numerous case studies are discussed along with satisfying outcomes that were acquired using MATLAB Simulink.

References

[1]. C. N. Bhende, S. Mishra and S. G. Malla, "Permanent Magnet Synchronous Generator-Based Standalone Wind Energy Supply System," in IEEE Transactions on Sustainable Energy, vol. 2, no. 4, pp. 361-373, Oct. 2011, doi: 10.1109/TSTE.2011.2159253.

[2]. M. W. Rahman, K. Velmurugan, M. S. Mahmud, A. Al Mamun and P. Ravindran, "Modeling of a stand-alone Wind-PV Hybrid Generation System Using (MATLAB/SIMULINK)," 2021 International Conference on Computing, Communication, and Intelligent Systems (ICCCIS), 2021, pp. 1000-1006, doi: 10.1109/ICCCIS51004.2021.9397194.

[3]. B. Singh and M. K. Singh, "Solar PV, PMSG -Wind Energy Conversion System and Battery Based Standalone DC Micro-Grid System," 2022 5th International Conference on Power Electronics and their Applications (ICPEA), 2022, pp. 1-6, doi: 10.1109/ICPEA51060.2022.9791165.

[4]. Malla, Siva Ganesh, Malla, Jagan Mohana Rao, Malla, Priyanka, Ramasamy, Sreekanth, Doniparthi, Satish Kumar, Sahu, Manoj Kumar, Subudhi, Pravat Kumar and Awad, Hilmy. "Coordinated power management and control of renewable energy sources based smart grid" *International Journal of Emerging Electric Power Systems*, vol. 23, no. 2, 2022, pp. 261-276. https://doi.org/10.1515/ijeeps-2021-0113

[5]. Malla, Priyanka, Malla, Siva Ganesh and Calay, Rajnish Kaur. "Voltage control of standalone photovoltaic – electrolyzer- fuel cell-battery energy system" *International Journal of Emerging Electric Power Systems*, 2022 early access. https://doi.org/10.1515/ijeeps-2022-0047

[6]. M. Bindi et al., "Comparison between PI and Neural Network Controller for Dual Active Bridge Converter," 2021 IEEE 15th International Conference on Compatibility, Power Electronics and Power Engineering (CPE-POWERENG), 2021, pp. 1-6, doi: 10.1109/CPE-POWERENG50821.2021.9501168.

[7]. S. Singh, S. Manna, M. I. Hasan Mansoori and A. K. Akella, "Implementation of Perturb & Observe MPPT Technique using Boost converter in PV System," 2020 International Conference on Computational Intelligence for Smart Power System and Sustainable Energy (CISPSSE), 2020, pp. 1-4, doi: 10.1109/CISPSSE49931.2020.9212203.

[8]. O. Flores-Acoltzi, I. Araujo-Vargas, N. Mondragón-Escamilla, M. Ponce-Flores and F. Valencia-Figueroa, "An optimized SVPWM scheme for a thirteen-level inverter," 8th IET International Conference on Power Electronics, Machines and Drives (PEMD 2016), 2016, pp. 1-6, doi: 10.1049/cp.2016.0189.

[9]. K.Dhineshkumar, C.Subramani, G.Prakash, "Analysis and comparison of 13 level inverter topology ", IOP Conf. Series: Journal of Physics: Conf. Series 1000 (2018) 012050 doi :10.1088/1742-6596/1000/1/012050

[10]. C Subramani, Dhineshkumar K, P Palanivel, "Design and Implementation of 13 Levels Multilevel Inverter for Photovoltaic System", IOP Conf. Series: Journal of Physics: Conf. Series 1000 (2018) 012047 doi :10.1088/1742-6596/1000/1/012047.

[11]. U. R. Muduli, B. Chikondra and R. K. Behera, "Space Vector PWM Based DTC Scheme With Reduced Common Mode Voltage for Five-Phase Induction Motor Drive," in IEEE Transactions on Power Electronics, vol. 37, no. 1, pp. 114-124, Jan. 2022, doi: 10.1109/TPEL.2021.3092259.

[12]. P. A. Dahono, A. Purwadi, Qamaruzzaman, **"An LC filter design method for single-phase PWM inverters",** *Proceedings of* ***International Conference on Power Electronics and Drive Systems*****, vol. 2, pp.** 571-576, **1995.**

[13]. D. Grenier, L. A. Dessaint, O. Akhrif, Y. Bonnassieux, and B. LePioufle, "Experimental Nonlinear Torque Control of a Permanent Magnet Synchronous Motor Using Saliency", *IEEE Transactions on Industrial Electronics*, vol. 44, no. 5, pp.680-687, Oct. 1997.

[14]. P.C. Krause, O. Wasynczuk and S. D. Sudhoff, "Analysis of electrical machinery and drive system", IEEE Press, 2002.

[15]. Siva Ganesh Malla and Priyanka Malla, "TS-Fuzzy Controller based Grid Connected Hybrid Renewable Energy Sources", International Journal of New Technologies in Science and Engineering (IJNTSE), Vol. 7, Issue. 7, pp. 1-13, July 2020.

[16]. O. Tremblay, L.-A. Dessaint and A. I. Dekkiche, "A Generic Battery Model for the Dynamic Simulation of Hybrid Electric Vehicles", *2007 IEEE-Vehicle Power and Propulsion Conference*, September 9-13, 2007 – Arlington/Texas, USA.

[17]. U. R. Muduli, K. A. Jaafari, R. K. Behera, A. R. Beig, K. A. Hosani and J. Y. Alsawalhi, "Predictive Battery SoC Control for Dual Propulsion Differential Four Wheel Drive Electric Vehicle," 2021 IEEE Energy Conversion Congress and Exposition (ECCE), 2021, pp. 1490-1495, doi: 10.1109/ECCE47101.2021.9595587.

[18]. M. Tarafdar Hagh, H. Taghizadeh and K. Razi, "Optimum control of multilevel inverters using Artificial Neural Networks," 2008 IEEE International Symposium on Industrial Electronics, 2008, pp. 2336-2341, doi: 10.1109/ISIE.2008.4677097.

[19]. D. O. Abdeslam, P. Wira, J. Merckle and D. Flieller, "Artificial neural networks to control an inverter in a harmonic distortion compensation scheme," 2008 IEEE International Symposium on Industrial Electronics, 2008, pp. 1879-1884, doi: 10.1109/ISIE.2008.4677022.

[20]. M. E. Haque, M. Negnevitsky and K. M. Muttaqi, "A Novel Control Strategy for a Variable-Speed Wind Turbine with a Permanent-Magnet Synchronous Generator", *IEEE Transactions on Industry Applications*, vol. 46, no. 1, pp. 331-339, Jan/Feb 2010.

[21]. M. E. Haque, K. M. Muttaqi and M. Negnevitsky, "Control of a Stand Alone Variable Speed Wind Turbine with a Permanent Magnet Synchronous Generator", *Proceedings of IEEE Power and Energy Society General Meeting*, pp. 20-24, July 2008.

[22] Sivachandran, P., Lakshmi, D., & Janani, R. (2015). Survey of maximum power point tracking techniques in solar PV system under partial shading conditions. ARPN Journal of Engineering and Applied Sciences, 10(1), 256-264.

[23] Lakshmi, D., Fathima, A., & Muthu, R. (2016). Simulation of the Two-Area Deregulated Power System using Particle Swarm Optimization. International Journal on Electrical Engineering & Informatics, 8(1).

[24] Sasilatha, T., D. Lakshmi, J. K. Vaijayanthimala, R. K. Padmashini, S. Priya, J. Padmapriya, and KS Kavitha Kumari. "Investigation of Hybrid Power System for Marine Applications." WSEAS Transactions on Power Systems 17 (2022): 207-217.

[25] R. K. Padmashini., N. Durai Murugan."Characterisation of Big Data Research in Applications of Health Care"Test Engineering and Management, Vol. 82: (2020)

[26] Deshpande, Soham G., and N. Bhasme. "Modeling and Simulation of Microinverter with Flyback Converter for grid connected PV systems." International Journal of Electrical and Electronics Engineering Research 7.4 (2017): 71-82.

[27] Kanchikere, Jayanna, A. K. Ghosh, and Kalyan Kumar. "Analysis of 80 KW grid connected rooftop solar power plant using SISIFO." Int. J. Mech. Prod. Eng. Res. Dev 8 (2018): 33-46.

[28] Rao, KV Govardhan, and P. Babu Rao. "A Novel Hybrid PV/FC Energy Management Scheme For Grid Connection And Islanded Operation Capabilities." International Journal Of Electrical & Electronics Engineering Research (IJEEER) 4.05 (2014): 13-26.

[29] Prakhya, Rajesh Kumar, and C. Krishna Reddy. "Comparison of Various Types of Rooftop Grid Connected Solar Plants: A Case Study." International Journal of Electrical and Electronics Engineering Research (IJEEER) 7.2 (2017): 11-22.

[30] Ashwin, J. S., and N. Manoharan. "Renewable energy based micro-grid system for power quality improvement." International Journal of Mechanical and Production Engineering Research and Development (IJMPERD) 8.1 (2018): 883-888.

[31] Mahela, O., and S. Ola. "Modeling and control of grid connected photovoltaic system: A Review." International Journal of Electrical and Electronics Engineering Research (IJEEER) 3.1 (2013): 123-134.